Measurement of MPD Thruster Erosion Using Surface Layer Activation

J.E. Polk,* W. von Jaskowsky,† A.J. Kelley,‡ and R. G. Jahn§
Princeton University, Princeton, New Jersey

An in-situ method for measuring MPD thruster component erosion has been developed and tested on two multimegawatt thruster configurations. The technique involves activation of selected areas on the components to be studied by precisely controlled high-energy ion beam bombardment. Monitoring the decrease in activity during thruster operation provides a precise, quantitative measure of the amount of material removed from the surface. In preliminary tests, erosion of the tungsten cathode occurred at all operating conditions, but a number of factors contributed to the lack of detectable erosion of the copper anode or the boron nitride insulator. These results indicate that cathode erosion is linearly related to the total charge transfer, but scatter in the individual test sequence erosion rate data prevents a more definitive conclusion. Nevertheless, a comparison of erosion data obtained at two different pulse lengths indicates that cathode material loss is generally independent of the number of pulse cycles. Work is continuing in a broad effort to refine the surface layer activation technique and to obtain a data base for additional thrusters.

Introduction

THE power level and longevity of magnetoplasmadynamic (MPD) thrusters are limited by electrode and insulator erosion. As part of a broadly based effort to assess erosion rates and to understand and model erosion processes, two in-situ erosion monitoring systems have been developed and applied to experimental thruster configurations.[1] The first technique, reported previously,[2] employed flush-mounted quartz crystal microbalances (QCM's) to measure boron nitride insulator erosion. The high sensitivity of the microbalance frequency to the crystal mass permitted an accurate measure of the loss of the sputter-deposited boron nitride surface layer, but its use was limited to low-temperature insulator surfaces and, therefore, provided no information about the erosion of other components in the thruster.

The second technique, which is the subject of this paper, involves bombardment of localized areas on the cathode, anode, and insulator to produce a slightly radioactive surface layer. A depth/activity calibration curve obtained from an identically irradiated and prepared test sample permits changes in the activity to be interpreted in terms of surface material loss. Not only does this technique provide the requisite submicron level accuracy, but, most importantly, it has wide applicability to a broad array of materials and operating conditions.[3,4]

This report provides a general summary of the surface layer activation (SLA) erosion monitoring method and presents the results obtained by application of the technique to the measurement of surface degradation of multimegawatt MPD thruster components. These test results have permitted tentative conclusions concerning general surface loss mechanisms.

Received Oct. 29, 1985; revision received July 18, 1986.

*Graduate Student, Electric Propulsion Laboratory.
†Research Engineer, Electric Propulsion Laboratory.
‡Senior Research Engineer, Electric Propulsion Laboratory.
§Dean, School of Engineering and Applied Science, Electric Propulsion Laboratory.

Experimental Apparatus and Procedure

The full-scale "benchmark" coaxial thruster configuration[5] shown in Fig. 1 was chosen for initial tests of the SLA technique and the half-scale flared anode thruster[6] pictured in Fig. 2 is currently being studied with this diagnostic method. In the benchmark thruster, a 2% thoriated tungsten cathode mounted on the centerline is separated from the annular copper anode plate by boron nitride and lucite insulators, which form the backplate and sidewalls of the thrust chamber. In the flared configuration, the annular copper anode forms the sidewalls of the thrust chamber, extending back to the boron nitride backplate that insulates it from the tungsten cathode in the center. In both designs, the argon propellant is delivered by a high-speed solenoid valve to both an annulus in the boron nitride backplate surrounding the cathode and a number of holes through the backplate arrayed in a circle about the cathode.

The thruster assembly, mounted for test in a fiberglass vacuum tank 1.8 m in diameter and 4.8 m long, as shown in Fig. 3, experiences prerun pressures of about 10^{-5} Torr. The arc current is provided by a 3000 μF pulse-forming network producing up to 30 kA in 1 ms rectangular pulses or up to 15 kA in 2 ms pulses at sustainable pulse rates up to 1 Hz.

As indicated in Figs. 1 and 2, spots 5 mm in diameter on the tungsten cathode, copper anode, and boron nitride backplate were activated by bombardment with a high-energy alpha or proton beam at the Princeton Cyclotron Facility. The backplates were irradiated where the QCM data indicated the erosion was most severe and the cathode spot was placed where high-current densities had been measured. To avoid irradiating a curved surface, the benchmark anode was bombarded on the flat face adjacent to the lip radius, which is subjected to the highest current density. The flared anode was irradiated on the cylindrical section upstream of the flare, near the current concentration measured at the beginning of the flare. The isotope and beam parameters listed in Table 1 were chosen on the basis of a number of considerations, all of which have had to be addressed to obtain meaningful results. The total dose and subsequent target surface disruption are limited by selecting the beam energy that corresponds to the maximum reaction cross section for the desired transmutation. Beam energy also determines the depth of penetration and therefore, the activity depth profile. In addition, specific isotopes to be used are chosen to have half-lives that are suffi-

ciently long to permit an adequate time for testing and to produce gamma ray spectra that are well-defined and distinct from those of other isotopes used in the experiment. The activity level is determined by the total amount of charge transfer and was chosen to produce a strong gamma signal and a density of activated material high enough to provide a detectable change in activity level due to erosion after a reasonable number of discharges (<1000). Moreover, the total activity had to be consistent with nuclear safety regulations and the desire to minimize the amount of radioactive material used in the experiment. With effort, all of these disparate factors can be simultaneously satisfied, as evidenced by the spectrum of Fig. 4 where the distinct, well-separated photopeaks produced by the three isotopes Os^{185} (tungsten), Zn^{65} (copper), and Be^{7} (boron nitride) are displayed.

The gamma radiation produced by the irradiated spots is only slightly attenuated by the surrounding thruster body and can thus be detected by a 5×5 in. NaI (T1) scintillator crystal mounted outside of the thruster. The photomultiplier tube mounted contiguous with the crystal provides a low noise output proportional to the gamma ray energy, which is converted to a spectrum via a multichannel analyzer. The spectra are analyzed by first subtracting the background from each of the three photopeaks using a linear approximation involving fitting a line to four points at each end of the particular range of interest (ROI), as illustrated in Fig. 5. The countrate is then determined from the collection time and the counts in each photopeak. This countrate, when normalized by the prefiring countrate and corrected for natural decay, is a direct measure of the existing activity level.

The eroded depth is determined by comparing this normalized activity level with the previously generated activity-depth calibration curves.[4] These depth profiles are obtained by precision lapping copper, tungsten, and boron nitride samples irradiated with the same beam parameters used to activate the actual thruster components. Profiles for the three materials are shown in Figs. 6–8, where the circles are from samples irradiated to about 1.5 μCi and the squares are from samples irradiated to about twice that level. The profiles are seen to be independent of the intensity of the activity and can be used with confidence to measure the mass loss from similar materials, provided the test item is irradiated in accordance with the conditions noted in Table 1.

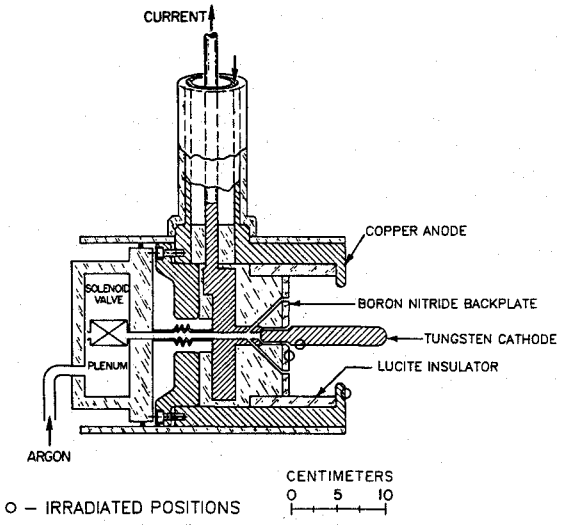

Fig. 1 Full-scale benchmark thruster.

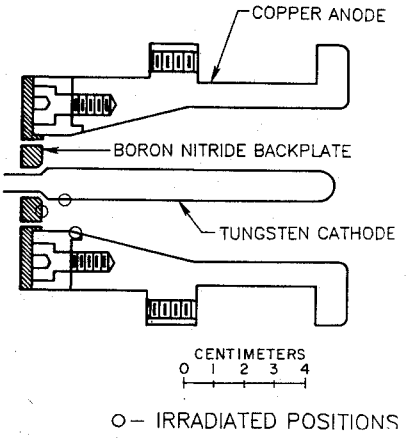

Fig. 2 Half-scale flared anode thruster.

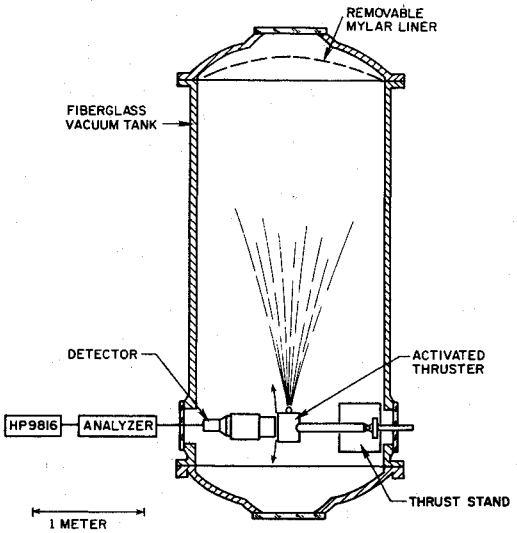

Fig. 3 Vacuum facility.

Table 1 Activation parameters

Parameter	Target W (cathode)	Target Cu (anode)	Target BN (backplate)
Isotope	Os^{185}	Zn^{65}	Be^{7}
Reaction	$^{183}W(\alpha,2n)^{185}Os$	$^{65}Cu(p,n)^{65}Zn$	$^{10}B(p,\alpha)^{7}Be$
Beam energy, MeV	23 alphas	4.25 protons	2.4 protons
Total charge	30.67[a]	57.35[a]	22.25[a]
on target, mC	64.80[b]	162.00[b]	69.60[b]
Activity level, μCi	1.41[a]	1.50[a]	0.74[a]
	3.67[b]	5.04[b]	2.92[b]
Production	0.046[a]	0.026[a]	0.033[a]
rate, μCi/mC	0.057[b]	0.031[b]	0.040[b]

[a]Full-scale benchmark thruster. [b]Half-scale flared anode thruster.

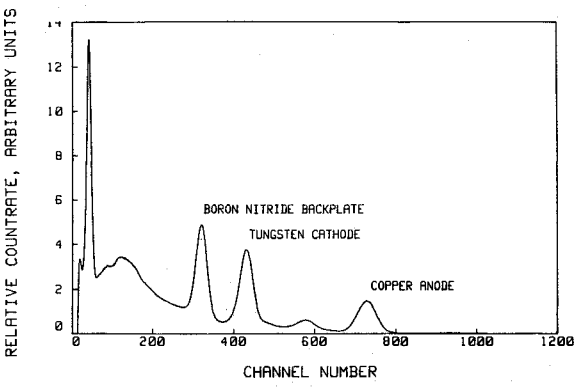

Fig. 4 Component spectrum.

Table 2 Test sequence and cathode erosion data summary ordered by current and depth range

Run	Discharges	Current, kA	Pulse length, ms	Depth range, μm	Erosion rate, μm/1000 discharges	Erosion rate, μm/10^5C
			Full-scale benchmark thruster			
7	4656	10	1	10.03–11.91	0.39	3.9
4	975	15	2	5.33–7.04	1.6	5.2
6	2849	15	1	8.27–10.03	0.68	4.5
8	3954	15	1	11.91–13.97	0.52	3.4
1	2478	23	1	1.10–3.12	1.0	4.5
3	620	23	1	4.42–5.33	1.6	6.4
5	2433	23	1	7.04–8.27	0.41	1.8
9	3832	23	1	13.97–15.20	0.34	1.5
2	2623	27	1	3.12–4.42	0.52	1.9
			Half-scale flared anode thruster			
1	629	12	1	0–8.03	—[a]	—[a]
2	672	12	1	8.03–8.22	0.13	1.1
3	802	12	1	8.22–10.32	—[a]	—[a]
4	2520	12	1	10.32–10.69	0.13	0.93
5	802	12	1	10.69–11.34	—[a]	—[a]
6	2423	12	1	11.34–11.66	0.18	1.3

[a]Discontinuities in curve.

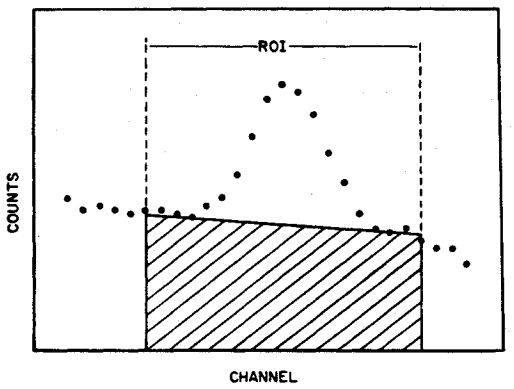

Fig. 5 Background stripping with a linear approximation.

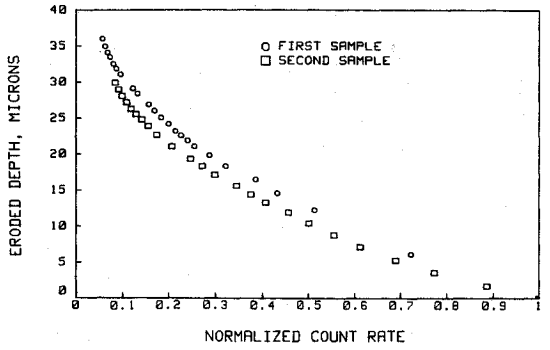

Fig. 6 Copper activity profile.

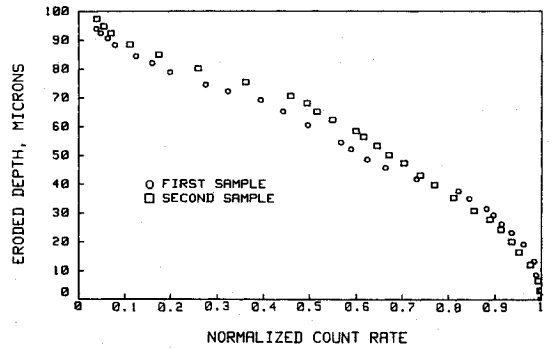

Fig. 7 Boron nitride activity profile.

Results and Discussion

Full-Scale Benchmark Component Erosion

An injected mass flow rate of 3 g/s was used throughout all of the individual test sequences noted in Table 2. The thruster testing involved 24,420 discharges representing a total charge transfer of 461,975 C. Four current levels (10, 15, 23, and 27 kA) were examined, with particular emphasis placed on the 23 kA discharges, which should have been near or above the thruster "onset current"; the characteristic current for a particular mass flow and geometry at which severe electrode and insulator ablation is observed. A pulse length of 1 ms was used for all except one test sequence in which 2 ms pulses at 15 kA were used to evaluate the influence of start/stop transients on erosion.

Although cathode erosion was measured at all current levels, no decrease in activity due to erosion was observed in the irradiated spot on the copper anode or on the boron nitride backplate. This contrasts with earlier QCM experiments that showed significant insulator ablation during operation above the onset current. These measurements indicated that for this thruster configuration onset occurs at about 22 kA during operation at 3 g/s, so the tests at current levels above 22 kA should have produced detectable erosion of the boron nitride. The onset current is usually identified as the current at which the magnitude of fluctuations in the terminal voltage reaches 10% of the mean voltage. As indicated by the data of Fig. 9, which show wise fluctuations in the current at which the 10% fluctuation, onset condition was measured, it is difficult to confirm whether any of the test points were actually above onset.¶ In addition, the depth calibration curve for boron nitride displayed in Fig. 7 indicates a relative insensitivity of

¶Terminal voltage data indicated that the mass flow rate was higher than the injected mass flow rate. Post-run visual inspection revealed that ablation of the lucite insulator used as the thrust chamber sidewall could have contributed a significant amount of mass to the discharge. This additional mass probably raised the onset current to a level beyond the maximum test currents. It must be concluded that the true mass flow rate and propellant composition for the test sequence are uncertain and could have fluctuated within broad limits during the experiment.

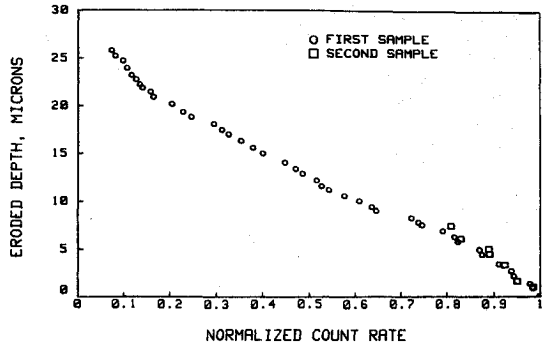

Fig. 8 Tungsten activity profile.

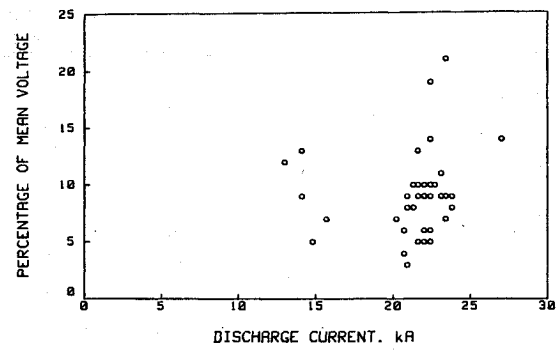

Fig. 9 Voltage fluctuations, full-scale benchmark thruster.

activity level with depth for approximately the first 10 μm. Therefore, although there were no measurable indications of gross insulator ablation, there may well have been some erosion present that was masked by the insensitivity of the technique in this regime. It must be concluded that the combination of operating condition variability and depth calibration insensitivity conspire to limit the results of this analysis to the general statement that it is not inconsistent with previous QCM observations.

The failure to measure erosion of the copper anode is more surprising. Not only did post-run visual inspection of the anode show heavy arc attachment damage to the radius of the anode lip, but a comparison of the copper and tungsten depth calibration curves of Figs. 6 and 8 shows them to be of comparably high sensitivity. Consequently, the erosion loss of submicron amounts of material from the activated spot would have produced detectable changes in the activity level. This permits the unambiguous conclusion that no mass removal occurred from the activated spot position. A possible explanation is that the highest current concentration occurs on the lip radius and not on the anode face, a conjecture supported by previous current mapping of a similar anode structure.[7]

The fact that cathode erosion is present at all current levels indicates that removal of cathode material is an inherent feature of MPD thruster operation, consistent with spectroscopic observations.[8] The plots of cathode erosion as a function of the total number of discharges (Fig. 10), and as a function of the charge transfer in megacoulombs (Fig. 11) indicate a roughly linear relationship between the eroded depth and the number of discharges or charge transfer. However, variations of erosion rate with current among the nine test sequences are apparent. Linear fits to the entire set of data from the nine tests give erosion rates of

$$0.582\ \mu\text{m}/10^3 \text{ discharges or } 3.33\ \mu\text{m}/10^5\ \text{C}$$

If the erosion is assumed to be uniform over the cathode surface, the mass loss rate would correspond to an erosion rate of 4.43 μg/C, a rate that is in good agreement with weight loss measurements.[9] The data points for each of the nine test sets produced very good linear fits, which are listed as erosion rates in columns 6 and 7 of Table 2. Comparison of these nine correlations, as shown in Fig. 12, indicates that the erosion rates from the different test sequences at 15 and 23 kA are widely scattered, masking any relationship between eroded depth and current level. Interestingly, the close linear fit apparent within each of the nine data sets argues against interpreting this scatter in terms of shot-to-shot mass flow fluctuations. These factors notwithstanding, there is now evidence for cathode erosion being controlled by current flow without a minimum threshold.

Also, the data obtained at 15 and 23 kA indicate that the erosion rate decreases with eroded depth. One possible explanation for this behavior is a variation in material properties with depth due to radiation damage sustained during activation of the spot, a factor to be studied as a part of our continuing effort to validate the SLA technique as a viable method of studying erosion. Finally, comparison of the data sets obtained at 15 kA with different current pulse lengths shows an erosion rate for the 2 ms run approximately twice that of the 1 ms runs, suggesting that the erosion rate may be more closely dependent on charge transfer than on the number of startup or decay transients.

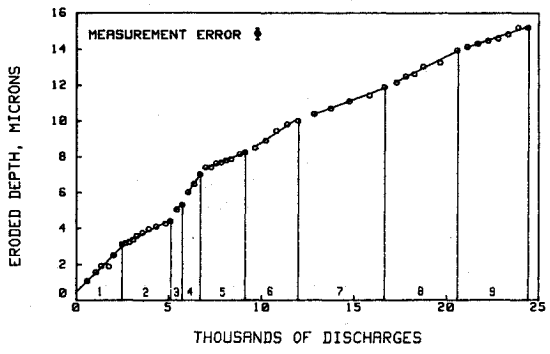

Fig. 10 Cathode erosion, full-scale benchmark thruster.

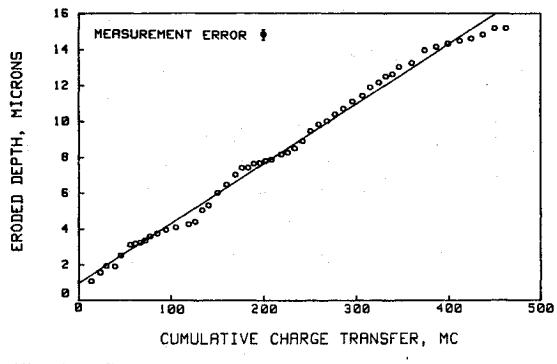

Fig. 11 Cathode erosion, full-scale benchmark thruster.

Flared Anode Thruster Component Erosion

Current testing with the half-scale flared anode thruster has been restricted to operation with argon propellant at a mass flow rate of 2.2 g/s and a current level of 12 kA, below the onset condition at ~22 kA. Although no erosion of the boron nitride backplate or the copper anode has been detected in this thruster either, a loss of material from the tungsten cathode has occurred during the 8650 discharges, as the plots of eroded depth as a function of number of discharges and charge transfer in Figs. 13 and 14 show. Examination of these plots reveals that the surface material loss is occurring in a markedly different fashion in this thruster. Unlike the smoothly varying curves of data from the benchmark thruster (Figs. 10 and 11), the curves from the flared anode thruster show regions of

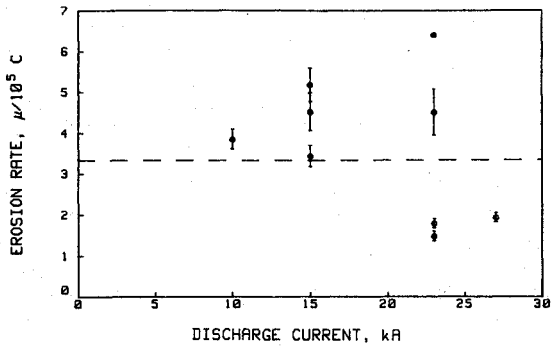

Fig. 12 Cathode erosion rates, full-scale benchmark thruster.

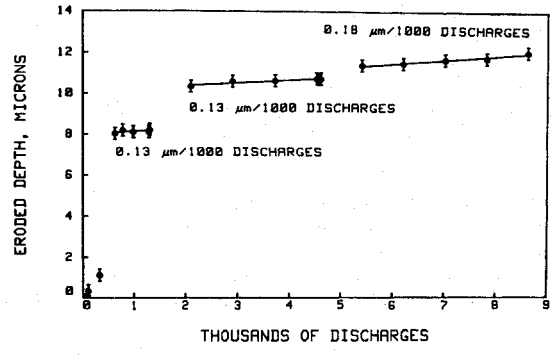

Fig. 13 Cathode erosion, half-scale flared anode thruster.

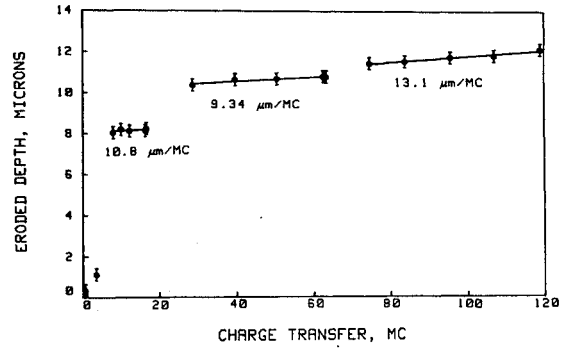

Fig. 14 Cathode erosion, half-scale flared anode thruster.

gradual, continuous variation in eroded depth separated by discontinuities where large amounts of material are lost in a relatively small number of discharges. The data obtained after about 2100 discharges (28,500 C) is much more regular than the data from the first several thousand shots and a linear fit to this data yields an erosion rate of

$$0.260 \text{ m}/10^3 \text{ discharges or } 1.92\ \mu/10^5 \text{ C}$$

which is comparable to that measured in the full-scale benchmark thruster. Again assuming uniform erosion on the entire cathode surface, this corresponds to an erosion rate of 1.10 μg/C. A better fit is possible, however, if this set of data is divided into two parts with a small discontinuity in the middle, as shown in Figs. 12 and 13. Fitting these two sections and the set immediately before produces the following erosion rates:

$$0.134\ \mu\text{m}/10^3 \text{ discharges, } 1.08\ \mu\text{m}/10^5 \text{ C, } 0.619\ \mu\text{g/C}$$

$$0.129\ \mu\text{m}/10^3 \text{ discharges, } 0.934\ \mu\text{m}/10^5 \text{ C, } 0.536\ \mu\text{g/C}$$

$$0.180\ \mu\text{m}/10^3 \text{ discharges, } 1.31\ \mu\text{m}/10^5 \text{ C, } 0.751\ \mu\text{g/C}$$

These results suggest the two mechanisms generally identified as dominant contributors to cathode degradation—the discontinuous loss of large quantities of cathode material and the more gradual removal of mass. The second type of erosion is similar to that observed in tests with the benchmark thruster and is probably due to the steady, evaporative loss of tungsten caused by Joule heating[10] or heating by ion impact[11] at the emitting sites. The first type of behavior could represent another erosion mechanism such as random spallation of relatively large molten drops[12,13] ("cathode spitting") or a manifestation of bombardment-induced radiation damage, such as preferential heating and ejection of a surface blister.

Summary

Localized areas on the copper anode, tungsten cathode, and boron nitride insulator of two different MPD thruster configurations were irradiated to produce a low level of nuclear activity. The change in activity of these regions with operation of the thruster permits a direct, quantitative measurement of surface material loss. The eroded depth was related to the observed decrease in activity by using previously measured profiles of normalized activity vs depth. Measurement of these depth profiles for the thruster materials at two different activity levels demonstrates that these profiles are independent of activity level.

Operation of the "benchmark" thruster for 24,420 discharges at different current levels and current pulse lengths produced no significant anode or insulator erosion. Although the anode was visibly eroded on the lip, the face of the anode where the activated spot was located did not ablate. The insulator probably remained undamaged because additional mass from ablation of a lucite sidewall prevented operation above the onset current where heavy insulator erosion is typical. In addition, insensitivity of the method to eroded depths less than 10 μm may have masked some erosion. Preliminary testing of the flared anode thruster configuration for 8650 discharges at a current below the onset current also produced no anode or insulator erosion.

In the benchmark thruster, cathode erosion was found at all current levels, indicating that this is an inherent feature of MPD operation. Erosion is linearly related to the charge transfer and occurs at a rate of 4.43 μg/C, under the assumption of uniform erosion over the cathode surface, which agrees well with various estimates based on weight loss measurements. Variation of erosion rate with current level was observed, but the data were scattered. This scatter may have been due either to fluctuations in the mass flow rate caused by lucite sidewall ablation or to changes in material properties with depth due to radiation damage. A test sequence at 15 kA with two different current pulse lengths indicates that the erosion rate is relatively insensitive to the number of startups and decay transients. Testing with the flared anode thruster has produced a similar erosion rate of 0.536–1.10 μg/C. In addition, these test indicate that another gross surface material loss mechanism exists, which may be a real erosion mechanism or a result of radiation damage. These data represent the first in-situ quantitative measurements of multimegawatt MPD thruster component erosion and serve as a guide to further research.

References

[1]Clark, K.E. and Jahn, R.G., "Magnetoplasmadynamic (MPD) Thruster Erosion Studies—Phase I," AF Contract F04611-79-C-0039, April 1983.

[2]Rowe, R., von Jaskowsky, W.F., Clark, K.E., and Jahn, R.G., "Erosion Measurements on Quasi-Steady MPD Thrusters," AIAA Paper 81-0687, April 1981.

[3]Conlon, T.W., "Doping Surfaces with Radioactive Atoms for Research and Industry," *Contemporary Physics*, Vol. 23, No. 4, 1982, pp. 353-369.

[4]Marks, L.M. Clark, K.E., von Jaskowsky, W.F., and Jahn, R.G., "MPD Thruster Erosion Measurement," AIAA Paper 82-1884, Nov. 1982.

[5]Kaplan, D.I. and Jahn, R.G., "Performance Characteristics of Geometrically-Scaled Magnetoplasmadynamic (MPD) Thrusters," Mechanical and Aerospace Engineering Dept., Princeton, NJ, Rept. 1492, 1982.

[6]Wolff, M.J., "A High Performance Magnetoplasmadynamic Thruster," Mechanical and Aerospace Engineering Dept., Princeton University, Princeton, NJ, Rept. 1632-T, 1983.

[7]Rudolph, L.R. and Jahn, R.G., "The MPD Thruster Onset Current Performance Limitation," Mechanical and Aerospace Engineering Dept., Princeton University, Princeton, NJ, Rept. 1491, Sept. 1980.

[8]Ho, D.D. and Jahn, R.G., "Erosion Studies in an MPD Thruster," Mechanical and Aerospace Engineering Dept., Princeton University, Princeton, NJ, Rept. 1515, 1981.

[9]Mori, K., Kurikaka, H., and Kuriki, I., "Effect of Electrode Configuration on MPD Arcjet Performance," IEPC Paper 84-11, July 1984.

[10]Daalder, J.E., "Joule Heating and Diameter of the Cathode Spot in a Vacuum Arc," Eindhoven University of Technology, Eindhoven, the Netherlands, Rept. TH-73-E-33, ISBN 90 6144-0335, 1973.

[11]Hantzsche, E., "On the Heat Sources of the Arc Cathode Spot," *Beitraege aus der Plasmaphysik,* Vol. 19, 1979, pp. 59-79.

[12]Udris, Y.Y., "On the Spraying of Droplets by the Cathode Spot in a Mercury Arc Discharge," *Investigations into Electrical Discharges in Gases*, edited by B.N. Klyarfel'd, Macmillan, New York, 1964, pp. 116-143.

[13]Utsumi, T. and English, J.H., "Study of Electrode Products Emitted by Vacuum Arcs in the Form of Molten Metal Particles," *Journal of Applied Physics,* Vol. 46, Jan. 1975, p. 126.